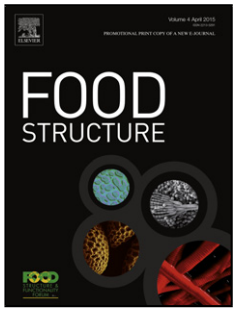

Title: Influence of adding a commercial phytosterol ester mixture on the 'equilibrium' crystallization behavior of palm oil

Authors: Eva Daels, Bart Goderis, Liselot Steen, Imogen Foubert

PII: S2213-3291(17)30158-2
DOI: https://doi.org/10.1016/j.foostr.2018.04.001
Reference: FOOSTR 97

To appear in:

Received date: 3-12-2017
Revised date: 9-4-2018
Accepted date: 20-4-2018

Please cite this article as: Daels E, Goderis B, Steen L, Foubert I, Influence of adding a commercial phytosterol ester mixture on the 'equilibrium' crystallization behavior of palm oil, *Food Structure* (2010), https://doi.org/10.1016/j.foostr.2018.04.001

Influence of adding a commercial phytosterol ester mixture on the 'equilibrium' crystallization behavior of palm oil

Eva Daels[a,b], Bart Goderis[c], Liselot Steen[b,d] and Imogen Foubert[a,b]

[a]Research Unit Food and Lipids, KU Leuven Kulak, Department of Molecular and Microbial Systems Kulak, Kortrijk, Belgium

[b]Leuven Food Science and Nutrition Research Centre (LFoRCe), Heverlee, Belgium.

[c]Polymer Chemistry and Materials, KU Leuven, Leuven, Belgium.

[d]Research Group for Technology and Quality of Animal Products, KU Leuven Technology Campus Ghent and Aalst, Ghent, Belgium.

[*]**Correspondence**: Imogen Foubert
Phone: +32 56 24 6997
E-mail: imogen.foubert@kuleuven.be

Graphical abstract

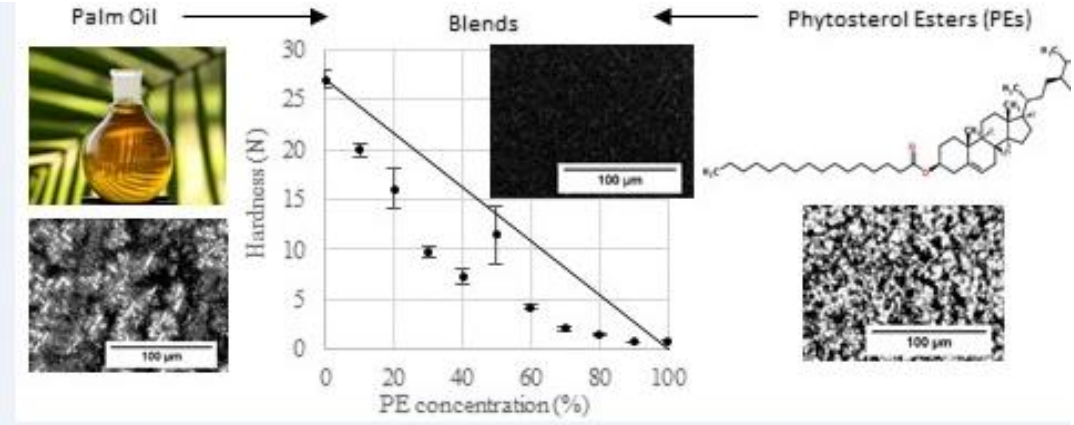

Highlights:

- Low phytosterol ester (PE) concentration: dilution effect
- High PE concentration: PEs crystallized in 1 or 2 crystal forms
- Addition of PEs led to a decrease in melting enthalpy and hardness of palm oil
- Binary system showed eutectic characteristics

Abstract

The objective of this study was to in depth investigate the 'equilibrium' state morphology and properties of crystals obtained after long-term isothermal crystallization and annealing of palm oil (PO) in the presence of different concentrations of phytosterol esters (PEs). A commercially available mixture of PEs was added to PO (0-100% PEs, 10% increment) and the effect of PE addition was analyzed with differential scanning calorimetry, X-ray diffraction, nuclear magnetic resonance, polarized light microscopy and texture analysis.

It was observed that PE addition had a major influence on each level of the crystalline structural hierarchy of PO in the 'equilibrium' state. The PE-PO binary system showed eutectic behavior. In case of a low PE concentration PEs itself did not crystallize but acted as a liquid oil diluting PO, while when added in a high concentration, PEs crystallized separately from PO. From a concentration of 40% PEs next to the β' crystals of PO also PE_x crystals were observed in the blends and from a concentration of 80% PEs additionally also the PE_y liquid crystals were

formed. The amount of PE_y in the blends with 80% and 90% PEs was however too low for the formation of the dense crystal structure as seen in pure PE. The crystal network structure of pure PO was lost after PE addition leading to a drop in the hardness.

Abbreviations

ΔH	melting enthalpy
DSC	differential scanning calorimetry
FA	fatty acid
NMR	nuclear magnetic resonance
PE(s)	phytosterol ester(s)
PLM	polarized light microscopy
PO	palm oil
SAXS	small angle X-ray scattering
SFC	solid fat content
TAG	triglyceride
T_{offset}	offset temperature of melting
WAXD	wide angle X-ray diffraction
XRD	X-ray diffraction

Keywords phytosterol esters, functional food, polymorphism, phase behavior, X-ray diffraction, differential scanning calorimetry

1. Introduction

Several commonly consumed food products, such as butter, margarine and chocolates contain an important amount of lipids, of which a substantial amount is present in the crystallized form. The crystallization behavior of lipids is of extreme importance in this type of food products. The macroscopic properties, such as spreadability, appearance and mouthfeel, snap of chocolate, texture, etc., strongly depend on the underlying lipid crystal network. When lipids

are cooled, they form primary crystals with specific shapes and sizes and with a characteristic polymorphism. These crystals aggregate through van der Waals attraction and clot to form clusters, which interact further, resulting in the formation of a continuous three-dimensional lipid crystal network. The number, size, shape and spatial distribution of crystals and clusters define the microstructure, which has an enormous influence on the macroscopic properties of lipid products. Each step in this structural hierarchy is influenced by the processing conditions such as cooling rate, crystallization temperature, agitation speed and storage time (Narine & Marangoni, 1999).

Palm oil (PO), derived from the mesocarp of the fruit of the oil palm tree (*Elaeis guineensis*), has surpassed soybean oil to be the most consumed vegetable oil in the world because of its unique physical properties (Tan & Nehdi, 2012). Because PO is semi-solid at ambient temperature, it is a very suitable trans-free main ingredient in e.g. margarines and shortenings to provide consistency, texture and structure. The offset temperature of melting (T_{offset}) of PO ranges between 32 and 40°C, which is very close to body temperature providing a desirable sensation upon being eaten (i.e. a good 'mouth feel'). Furthermore it tends to induce the formation of rather stable needle-shaped (5 – 7 µm) β' crystals which give a smooth and glossy texture to margarines and shortenings (Pande, Akoh, & Lai, 2012; Kiyotaka Sato, 1999; Tan & Nehdi, 2012). β crystals are much longer (20 – 30 µm) than β' crystals and are not desirable as they would produce a margarine that is brittle, grainy, sandy, oiled out and has a dull appearance (Miskandar, Man, Yusoff, & Rahman, 2005).

Phytosterols include over 250 different compounds including plant sterols and their hydrogenation products, plant stanols. The richest natural sources of phytosterols are vegetable oils followed by cereal grains and nuts, but they can also be extracted from vegetable oils or tall oil in order to be used in pharmaceutical, cosmetic and food applications (Fernandes & Cabral, 2007; Piironen, Lindsay, Miettinen, Toivo, & Lampi, 2000). Because their chemical structure is very similar to that of cholesterol phytosterols have the ability to reduce circulating cholesterol concentrations when an optimal intake is reached. A meta-analysis of 124 trials showed that a 6-12% reduction in the blood levels of LDL-cholesterol can be obtained with an optimal intake of phytosterols of 0.6-3.3 g/day (Ras, Geleijnse, & Trautwein, 2014). Given the fact that the average daily intake of plant sterols in adults only reaches between 150 and 400 mg/day, phytosterols have to be administered via the diet in a higher concentration in order to benefit from their health-promoting properties since they are not synthesized in the body (Ntanios, 2001). One possible administration method is esterification of phytosterols with a fatty acid to obtain phytosterol esters (PEs) which facilitates their incorporation into lipid

containing foods (Ostlund, 2007). PEs are currently already being used as a food ingredient in modern functional food formulations. Margarines and table spreads are ideal vehicles, although cream cheese, salad dressings, and yogurts are also used as delivery systems (Vaikousi, Lazaridou, Biliaderis, & Zawistowski, 2007). The PE concentration that is applied in the fat phase in these products is in the range of 10 to 50% depending on the product type (e.g. light margarine, margarine with butter or olive oil, etc.).

Addition of PEs to lipid (containing food products) may influence its crystallization behavior and may thus lead to problems occurring during the production process or with the macroscopic properties of the end product (Rodrigues, Torres, Mancini-Filho, & Gioielli, 2007; Vu, Shin, Lim, & Lee, 2004). Fundamental research on this topic is however very scarce. One study showed that self-made PEs added to liquid corn oil caused unwanted crystallization above a certain threshold concentration (Vu et al., 2004) and another research group investigated how the crystallization behavior of milk fat was changed by blending with a commercial mixture of PEs (Rodrigues et al., 2007). They showed that on addition of PEs milk fat has a softer consistency and a lower solid fat content. In a previous study (Daels, Foubert, & Goderis, 2017) the non-isothermal crystallization and melting behavior of a commercial PE mixture in blends with PO was investigated with differential scanning calorimetry (DSC) and time-resolved synchrotron X-ray diffraction (XRD) measurements. Two different crystal structures were identified in the commercial PE mixture. The crystal structure designated PE_x needed a very high degree of supercooling to induce nucleation and was probably composed of stearic and palmitic acid esterified PEs. The crystal structure designated PE_y crystallized without supercooling, was liquid crystalline and probably predominantly contained oleic acid esterified PEs. Such formation of liquid crystalswas also reported by Leeson et al. (2002) in short-chain saturated and long-chain unsaturated PEs, but was absent in long-chain saturated PEs. The PE-PO blends in the study of Daels et al. (2017) showed eutectic behavior as the PEs and PO crystallized separately from each other and no new crystal structures were formed. The occurrence of different polymorphic forms during cooling and heating of the PE-PO blends was mapped as a function of temperature and PE concentration on two morphology maps.

It is hard to predict whether or not PE addition gives any desired properties to the end product based on these non-isothermal experiments as Daels et al. (2017) did not produce equilibrium conditions and did not give direct information on microstructure or macroscopic assets such as the hardness which is a very crucial characteristic of food products. Therefore in this study the influence of the addition of a commercially available mixture of PEs was analyzed at each structural level of the crystallization of PO being primary crystallization, polymorphism,

network formation and textural properties. To do so many different experimental techniques were applied including DSC, XRD, nuclear magnetic resonance (NMR), polarized light microscopy (PLM) and texture analysis. The effect of PE addition was tested on the properties of PO crystals in a kinetically stabilized state obtained after long-term isothermal crystallization and annealing. This kinetically stabilized state is from now on denoted as the 'equilibrium' state.

Materials and methods

1.1. Sample preparation

PO and a commercial PE mixture were donated by Unilever (Vlaardingen, The Netherlands). The commercial PE mixture had a degree of esterification of 97.7 ± 1.1% as was confirmed by solid phase extraction performed as described in Panpipat, Xu, & Guo, 2013. Table 1 shows the sterol composition of the commercial PE mixture as measured by the method described in Ryckebosch, Bruneel, et al. (2012). The FA composition of PO and the commercial PE mixture as determined by the method described in Ryckebosch, Muylaert, & Foubert (2012) are reported in Table 2. The FA composition of PO is in the range that is reported in literature (Tan & Nehdi, 2012). Finally Table 3 depicts the triglyceride (TAG) composition of the PO which was analyzed in a high-performance liquid chromatograph (HPLC) (Waters, Belgium) coupled with a refractive index detector (Waters, Belgium). The applied column was a NOVA-Pak C18 (4 µm, 150 × 3.9 mm; Waters, Belgium) at 30°C and acetonitrile–acetone (37.5:62.5, vol/vol) was used as the mobile phase. PO was solubilized in a chloroform/methanol mixture (1:1, vol/vol) at a concentration of 20 mg/mL. Samples were injected in duplo in the quantity of 20 µL. The TAG composition of PO was also in good agreement with the literature (Tan & Nehdi, 2012).

1.2. Blend preparation

Nine binary blends of PEs and PO were prepared with a PE concentration of 10 to 90% with composition intervals of 10%. The samples were prepared after complete melting of the pure lipids at 80°C for 30 min under continuous stirring and the blends were stored at -20°C.

1.3. Crystallization to the 'equilibrium' state

In this study the effect of PE addition on PO crystallization in the 'equilibrium' state was examined. First the samples were melted at 80°C during 15 min and thereafter put in a water bath at 10°C for rapid cooling (at about 5°C/min). In accordance with the existing literature (AOCS, 1997a), a time-temperature profile of 48h at 10°C was used to bring the samples in the

'equilibrium' state. It was observed that the DSC melting enthalpy and the peak maximum of the melting curve of pure PO and PEs indeed did no longer change significantly when holding at that temperature for longer than 48h (times up to 7 days were tested) (detailed results not shown). The described tempering of the samples was performed in a water bath.

1.4. Solid fat content by NMR

The solid fat content (SFC) of the samples in the 'equilibrium' state was measured with a pulsed NMR spectrometer (Mini-spec mq20; Bruker, Germany) using the direct method as described by AOCS (1997b). Calibration was performed by using three standards supplied by Bruker containing 0.0, 31.3, and 74.0% solids. Determinations were carried out in triplicate. For the pure PEs one extra SFC measurement was performed at 25°C, after the measurement at 10°C and subsequent heating to 25°C and holding at 25°C for 1h.

1.5. Melting profile by differential scanning calorimetry

The DSC experiments were performed with a DSC type Q2000 (TA Instruments, Brussels, Belgium) equipped with an autosampler. A baseline calibration was performed using sapphire and indium, an empty pan was used as a reference and nitrogen was the purge gas. About 10-20 mg of the melted samples was sealed into Tzero hermetic aluminum pans (TA Instruments, Brussels, Belgium). After reaching the 'equilibrium' state, the samples were heated at 20°C/min to 80°C to obtain the melting profile. For each sample, at least five repetitions were evaluated. The melting enthalpy (ΔH), i.e. the amount of heat absorbed during melting, was calculated by integration of the melting curve using a horizontal baseline. The offset temperature of melting (T_{offset}) of different peaks in the melting curve was determined as the inflection point of the melting peak at the high temperature side of the peak, according to Timms (2003).

1.6. X-ray diffraction

A Xenocs Xeuss X-ray camera (Xenocs, Sassenage, France) equipped with a Mar345 image plate detector (MARresearch, Norder-stedt, Germany) was used for taking X-ray scattering patterns of a selection of samples in the 'equilibrium' state: the PE-PO blends with 20, 40, 60 and 80% PEs and pure PO and PEs. The GeniX 3D Molybdenum ultra-low divergence X-ray beam source had a power of 50 kV (1 mA) giving a constant intensity beam of 0.7107 Å. About 25-30 mg of melted sample was sealed into Tzero hermetic aluminum pans (TA Instruments, Brussels, Belgium). After reaching the 'equilibrium' state the samples were placed on a temperature-controlled Linkam DSC600 stage (Linkam Scientific Instruments, Surrey, UK) in

front of the beam. Combined small-angle X-ray scattering (SAXS) and wide-angle X-ray diffraction (WAXD) patterns were recorded at a constant temperature of 10°C. All X-ray patterns were processed with Conex software also using an empty DSC pan measurement and a calibration measurement with a silver behenate sample (Gommes & Goderis, 2010).

1.7. Polarized light microscopy

The microstructure of the samples was studied by means of a polarized light microscope Olympus BX51 (Olympus Optical Co. Ltd., Tokyo, Japan) equipped with a digital camera Infinity 2 (Lumenera corporation, Ontario, Canada). A drop of melted sample was transferred onto a glass slide using a capillary tube and covered with a pre-heated covering slide. After reaching the 'equilibrium' state the samples were placed on a temperature-controlled Linkam PE120 stage set at 10°C (Linkam Scientific Instruments, Surrey, UK). Images were taken at a magnification of 100x or 200x using the Infinity capture software (Lumenera Corporation, Ottawa, Canada).

1.8. Hardness

Texture analyses of the nine PE-PO blends and pure PO and PEs was performed using a Lloyd Texture Analyzer (Model LF plus, Lloyd Instruments Ltd, Fareham, Hampshire, UK). Plastic cans with diameter 30 mm and height 70 mm were filled with 16 g sample. Force-distance deformation curves of the samples in the 'equilibrium' state were obtained using a 100 N load cell and a cylindrical probe (diameter 6 mm). The probe penetrated the lipid at a constant speed of 10 mm/min to a distance of 10 mm. The hardness (N) is defined as the maximum force required to penetrate the sample 10 mm. For each sample, four repetitions were evaluated.

1.9. Statistical analysis

The data were statistically analyzed by one-way ANOVA with SigmaPlot version 11.0 (Systat Software, Drunen, The Netherlands). Furthermore Tukey tests were applied to determine significant differences between the mean values of the different blends. A significance level of 0.05 was used throughout.

2. Results and Discussion

2.1. Pure palm oil

2.1.1. Solid fat content by NMR

The obtained value of the SFC of pure PO in the 'equilibrium' state was 52.5 ± 0.1%, which is within the typical range for SFC values of PO at 10°C reported in literature (Tan et al., 2012; Pande, Akoh & Lai, 2012).

2.1.2. Melting profile by differential Scanning Calorimetry

The melting curve of pure PO in 'equilibrium' shown in Figure 1 had one, rather broad peak with a peak maximum at about 30°C and a small shoulder on the high temperature side. The calculated T_{offset} of the pure PO was 38.7 ± 0.2°C and ΔH was 57.6 ± 0.5 J/g. The existence of one broad peak indicated that compound crystals, i.e. crystals with different types of triglycerides (TAGs) together (Moziar, DeMan, & DeMan, 1989), were formed, which is probably due to the high cooling rate (more than 5°C/min) obtained in the tempering procedure (Martini et al., 2002). The melting range of the obtained crystals indicated the existence of β' crystals (Sato, 2001; Verstringe et al., 2013a), which is according to literature the expected polymorphic form after tempering at 10°C since PO is a β'-tending lipid (Miskandar et al., 2005; Rousseau, Marangoni, & Jeffrey, 1998). The small shoulder on the high temperature side of the melting curve was reported by several other authors (Calliauw et al., 2010; Man, Haryati, Ghazali, & Asbi, 1999) but their suggested explanations for the shoulder were never really proven. To be sure if the shoulder was caused by (i) a polymorphic transition of β' to β during heating, (ii) a polymorphic transition of β' to β during tempering or (iii) the melting of some compound crystals richer in high melting trisaturated TAGs as was already suggested in literature (Calliauw et al., 2010; Man et al., 1999) some extra tests were performed on the pure PO after it reached the 'equilibrium' state. A variation of the heating rate (0.5, 1, 5, 10 and 20°C/min) had no influence on the shape of the melting curve of pure PO demonstrating that the shoulder was not due to a polymorphic transition of β' to β during heating (detailed results not shown). Furthermore when the tempering of PO was interrupted after several different time intervals (2h, 4h, 16h and 48h) to melt the sample at a heating rate of 20°C/min, the same shoulder was already present in the melting curves, which demonstrates that the shoulder could also not be related to the polymorphic transition of β' to β during tempering (detailed results not shown). Therefore the shoulder was most probably caused by the melting of some compound crystals richer in high melting trisaturated TAGs (mainly PPP and PPS).

2.1.3. X-ray diffraction

Figure 2 shows the wide angle X-ray diffraction (WAXD) and small angle X-ray scattering (SAXS) patterns of pure PO in the 'equilibrium' state. The SAXS pattern of pure PO showed

one main peak at 2θ = 0.96° (d = 42.2 Å) and a second much smaller peak at 2θ = 2.9° (d = 14.6 Å). These peaks correspond to the first (42.2 Å) and third order (14.6 Å) reflections of a 2L packing (Kiyotaka Sato, 1999). The WAXD pattern showed one medium peak at 2θ = 10.53° (d = 3.91 Å) and two strong peaks at 2θ = 9.73° (d = 4.19 Å) and 2θ = 9.43° (d = 4.32 Å). These short spacings are characteristic for the orthorhombic subcell stacking of PO in a β'-polymorph (Kiyotaka Sato, 1999; Verstringe et al., 2013; Yap, DeMan, & DeMan, 1989). Based on the DSC and XRD results of pure PO reported by Daels et al. (2017) it can be stated that these β' crystals consist of disaturated and trisaturated TAGs and that they compose the so-called high-melting fraction also called stearin fraction of PO and that they are formed by a polymorphic transition of α-crystals during tempering.

2.1.4. Polarized light microscopy

As can be seen in Figure 3 the microstructure of pure PO showed the typical network of spherulites which are themselves aggregates of needle-shaped crystals (Peyronel & Marangoni, 2014; Rodrigues et al., 2007; Rousseau et al., 1998). As could be expected many small crystals were formed due to the rather high cooling rate (Martini et al., 2005).

2.1.5. Hardness

With the texture analysis a hardness of 27.0 ± 0.1 N was obtained for pure PO.

2.2. Pure commercial phytosterol ester mixture

2.2.1. Solid fat content by NMR

The SFC of the pure PEs analyzed by NMR at 10°C was 62.3 ± 0.3%, which corresponds with the value reported by Rodrigues et al. (2007) for a commercial PE mixture that was also highly unsaturated (more than 85% of the FA were unsaturated). The SFC of the pure PEs at 25°C was 17.7 ± 0.1%, which is much lower than the SFC of the pure PEs at 10°C. This could be expected from the morphology map of heating reported in a previous study of Daels et al. (2017). The morphology map shows that at 10°C the two ordered structures of PEs, being PE_x and PE_y, can be expected, while at 25°C only the PE_x form will remain. Therefore it can be concluded that the high SFC value of the pure PEs at 10°C is dominated by the presence of PE_y liquid crystals, rather than of PE_x crystals. As was demonstrated by Daels et al. (2017) PE_y is liquid crystalline, instead of truly crystalline. However, since NMR measures mobility rather than true crystallinity, liquid crystals are taken for a solid phase during the NMR measurement leading to a high SFC value (AOCS, 1997b).

2.2.2. Melting profile by differential scanning calorimetry

The melting curve of the pure PEs shown in Figure 1 has two peaks: a sharp low-melting peak with a maximum at 16°C and a very broad high-melting peak between 25 and 45°C. Based on the morphology map of heating reported in a previous study of Daels et al. (2017), the low-melting and high-melting peaks could be attributed to the melting of respectively PE_y and PE_x. The calculated T_{offset} of the pure PEs was 45.6 ± 0.5°C and ΔH was 9.0 ± 0.8 J/g. In contrast to the observed SFC of the pure PEs being higher than that of pure PO, the ΔH of the pure PEs was much lower than that of pure PO (Figure 4). The low ΔH of the pure PEs is due to the structure of PE_y being liquid crystalline which generally leads to a low ΔH value (Ginsburg, Atkinson, & Small, 1984). It is for example reported in literature that the mesophase of β-sitosteryl linoleate, which is the main constituent in the commercial PE mixture used in this study, also has a very low ΔH of only 5.1 J/g (Leeson & Flöter, 2002).

2.2.3. X-ray diffraction

When looking at the XRD data of the pure PEs in Figure 2, the WAXD pattern showed a very broad peak at 2θ = 7.67° (d = 5.31 Å) and eight smaller peaks at 2θ = 5.36° (d = 7.60 Å) 2θ = 6.68° (d = 6.10 Å), 2θ = 6.86° (d = 5.94 Å), 2θ = 8.18° (d = 4.98 Å), 2θ = 8.68° (d = 4.70 Å), 2θ = 8.96° (d = 4.55 Å), 2θ = 9.71° (d = 4.19 Å) and 2θ = 10.72° (d = 3.82 Å). The peaks at 6.10 Å and 5.94 Å were very sharp, while the one at 4.19 Å was rather broad and was probably composed of two partially overlapping peaks. In the SAXS pattern one very intensive peak was observed at 2θ = 1.14° (d = 35.8 Å) and three rather small and broad peaks were detected at 2θ = 0.73° (d = 55.8 Å), 2θ = 1.46° (d = 27.5 Å) and 2θ = 2.23° (d = 14.1 Å). Based on a previous study the SAXS peak at 35.8 Å and the WAXD peak at 5.31 Å could both be linked to the ordered structure of PE_y, while the other short and long spacings corresponded to PE_x (Daels et al., 2017).

2.2.4. Polarized light microscopy

PLM of the pure PEs revealed a dense crystal structure, similar to that observed by Rodrigues et al. (2007) for a commercial PE mixture after storage at 10°C. The network had an irregular structure which is different from what is normally seen in TAG lipids since the crystals were not needle-shaped or organized into spherulites. The remarkable microstructure was typical for the presence of liquid crystals and was therefore caused by the presence of PE_y. In general mesophases are strongly birefringent and thus visible through PLM (Foubert, Dewettinck, Van de Walle, Dijkstra, & Quinn, 2007; Ginsburg et al., 1984).

2.2.5. Hardness

The observed hardness of the pure PEs was 0.9 ± 0.1 N, which is very low compared to pure PO. The low hardness despite the high SFC and high density of the crystal network is caused by the presence of liquid crystals since they generally consist of two-dimensional layers of ordered molecules that can move over one another, negatively affecting the hardness (Dierking, 2003). A similar observation was reported by Rodrigues et al. (2007) who also detected a low consistency in a commercial PE mixture with a high SFC and a dense crystal network. Different from what is generally observed in TAG lipids (Braipson-Danthine & Deroanne, 2004; Danthine & Deroanne, 2003; Miskandar et al., 2005; Vereecken, Foubert, Smith, & Dewettinck, 2007), hardness of the pure PEs is therefore not correlated with SFC, but only with ΔH and this due to the presence of a liquid crystalline phase in the form of PE_y.

2.3. Blends of the commercial phytosterol ester mixture and palm oil

2.3.1. Solid fat content by NMR

Figure 5 shows the SFC of the PE-PO blends as a function of the PE concentration. Next to that, three straight lines were added to Figure 5: the black solid line representing the theoretical value of SFC if PO would have been blended with a fully liquid oil, instead of PEs, the grey solid line representing the theoretical value of SFC if PE_x would have been blended with a fully liquid oil, instead of PO and the black dotted line showing the theoretical value of the SFC of the PE-PO blends supposing the PE solids consist only of PE_x. The latter one is thus the sum of the two dotted lines. When adding up to 50% PEs, the SFC of PO decreased almost perfectly linearly ($R^2 = 0.991$) upon PE addition, although the pure PEs had a higher SFC than pure PO. Moreover, the decrease in SFC of PO was equal to the proportion of added PEs (as indicated by the black solid line in Fig. 5) which demonstrates that PEs did not crystallize up to a concentration of 50%, but instead acted as a liquid oil diluting PO.

From a PE concentration of 60% the SFC values of the blends all lie clearly above the black solid line indicating that next to PO also PE crystallized in the blends, more specifically in the form of PE_x. It seems that in the blends of 80% PEs or less no PE_y crystals were formed since the SFC values still lie under the black dotted line. Only from a concentration of 90% PEs the SFC value was positioned above the black dotted line which indicates that also PE_y liquid crystals were formed in the blends next to PO and PE_x crystals.

2.3.2. Melting profile by differential scanning calorimetry

In the melting curves of the PE-PO blends shown in Figure 1 it can be seen that when the PE concentration increased, the total peak area gradually decreased, while the peak maximum of

the PO melting peak remained almost constant. From a PE concentration of about 50% onwards the endothermic peak was stretched out at the high temperature side. This extra plateau-shaped peak became bigger with an increasing PE concentration and was most probably due to the melting of PEs, since T_{offset} of the pure PEs is higher than that of pure PO.

In Figure 4 ΔH of the PE-PO blends was plotted as a function of the PE concentration together with three straight lines. The black solid line represents the theoretical value of ΔH if PO would have been blended with a fully liquid oil, instead of PEs. The grey solid line on the other hand represents the theoretical value of ΔH if the PEs would have been blended with a fully liquid oil, instead of PO and the black dotted line is the sum of the two previous ones showing the theoretical value of ΔH of the PE-PO blends supposing both components crystallized. A linear ($R^2 = 0.998$) decrease in ΔH of PO was observed when 10 up to 90% PEs was added. Moreover, similar as observed for SFC, the decrease of ΔH in the PE-PO blends was equal to the proportion of added PEs (as indicated with the black solid line in Fig. 2) revealing a dilution effect of the PEs, which acted as a liquid oil over the whole PE concentration range. Nevertheless there should be PE_x crystals present from a concentration of 60% PEs as demonstrated by the NMR results and by the theoretically expected values of ΔH for the blends with 60% PEs or more (as indicated with the black dotted line in Fig. 2) which was clearly higher than the experimentally obtained values.

T_{offset} of the blends as reported by Daels et al. (2017) and measured by synchrotron XRD are indicated by the grey solid line in Figure 1 and agree with the values of T_{offset} if they would have been visually determined based on the shape of the DSC curves. At some PE concentrations T_{offset} of the blends was clearly lower than both T_{offset} of pure PO and the pure PEs indicating eutectic behavior of the PE-PO binary system. The eutectic phase behavior was due to the PEs and PO being immiscible in the solid state because of their difference in molecular shape prohibiting the formation of compound crystals. Rodrigues et al. (2007) also observed eutectic behavior in blends of a highly unsaturated commercial PE mixture with milk fat.

2.3.3. X-ray diffraction

When looking at the XRD patterns of the PE-PO blends (Figure 2), only peaks with the same spacings as in the pure components were present. Since no new peaks at other spacings occurred in the XRD patterns, it can be concluded that no new crystal structures were formed in the PE-PO blends and the plots are thus superpositions of the already discussed SAXS and WAXD patterns of the pure substrates. In the SAXS and WAXD patterns of the PE-PO blends with

20% PEs only the typical PO peaks appeared, although smaller. From a concentration of 40% PEs next to the typical PO peaks also PE_x peaks were detected in the WAXD patterns. However in SAXS they were only found when zooming in very closely since the intensity of the PE_x peaks was very low in this concentration range. At a PE concentration of 80% the typical PE_y peak was seen in SAXS, although with a very low intensity. The typical PE_y peak in WAXD was not observed since in general in WAXD patterns the noise is bigger compared to SAXS patterns and the PE_y WAXD peak is a small and broad peak anyway while the PE_y SAXS peak is very strong. So in this blend next to PO and PE_x crystals also PE_y liquid crystals were formed, however most probably in a very low amount because of the very low intensity of the SAXS peak and since the presence of PE_y was not reflected in the results of the NMR analyses (see section 3.3.1). The XRD results of the 80% PE blend also indicate that even at high PE concentrations PO could still form a small amount of crystals. The morphology map of heating reported by Daels et al. 2017 shows that in the 80% PE blend PE_y has already fully cleared at a temperature of 2.9°C in contrast to our results which show that PE_y was present in that blend at 10°C. The slope of the curve of T_{offset} of PE_y as a function of the PE concentration is however rather steep around 80% PEs in the morphology map of heating, leading to a much higher T_{offset} of PE_y when the PE concentration is only slightly higher.

2.3.4. Polarized light microscopy

Blends with 10 to 40% PEs presented a similar crystal structure as pure PO, although with less and smaller spherulites when the PE concentration was higher. In the blends with 50 to 90% PEs only very little and very small granular crystals were visible. From the previous results for the PE-PO blends it was demonstrated that in the 80% and 90% PEs blends liquid crystals in the form of PE_y were formed in a very small amount. Probably the amount of PE_y was too low for the formation of a dense crystal network structure as was observed for the pure PEs.

2.3.5. Hardness

PE addition had a major influence on the hardness of PO as is shown in Figure 6. The black solid line represents the theoretical value of the hardness if PO would have been blended with a fully liquid oil, instead of PEs. When adding up to 70% PEs, the hardness of PO decreased strongly as a function of the PE concentration. When adding more than 70% PEs the hardness of the PE-PO blends reached a more or less constant value which was very low and in the same order of magnitude as the hardness of the pure PEs. The hardness of all the PE-PO blends was lower than the theoretical value in case PO would have been blended with a liquid oil. So in contrast to the SFC and ΔH results of the PE-PO blends, the decrease of the hardness as a

function of the PE concentration was much stronger than a dilution effect. This clearly shows that the crystal network structure of pure PO was lost after PE addition leading to a drop in the hardness.

3. Conclusions

It could be concluded that addition of PEs to PO (containing products) will influence the crystallization properties. In industry this may lead to problems occurring during the production process or with the macroscopic properties of the end product. In the PE concentration range that is usually applied in industrial applications (up to 40% PEs) the PEs negatively affected the SFC, ΔH, network structure and hardness, one of the key factors that determine the macroscopic characteristics of the food product. When applying this blend composition in a product, additional adaptations on the composition level will have to be made in order to compensate for the loss in hardness.

Acknowledgements

The authors express their sincere thanks to Annelien Rigolle (Puratos, Groot-Bijgaarden, Belgium) for her help with the DSC and microscopy analyses and to Olivier Verkinderen (KU Leuven, Leuven, Belgium) for his assistance with the X-ray diffraction measurements. We also want to thank Jeroen Maes, Peggy Dijckmans and Wim De Greyt (Desmet Ballestra, Zaventem, Belgium) for the use of the NMR instrument and their help with the SFC analyses and for performing the TAG analyses. Unilever (Vlaardingen, The Netherlands) is acknowledged for providing palm oil and the commercial phytosterol ester blend. This research did not receive any specific grant from funding agencies in the public, commercial, or non-for-profit sectors. The authors have declared no conflict of interest.

References

AOCS. (1997a). Official method Cc 3-25: Sofenting point. In *Official methods and recommended practices of the American Oil Chemists' Society*.

AOCS. (1997b). Official method Cd 16b-93: Solid fat content (SFC) by low-resolution nuclear magnetic resonance - The direct method. In *Official methods and recommended practices of the American Oil Chemists' Society*.

Braipson-Danthine, S., & Deroanne, C. (2004). Influence of SFC, microstructure and polymorphism on texture (hardness) of binary blends of fats involved in the preparation of industrial shortenings. *Food Research International*, *37*, 941–948.

Calliauw, G., Fredrick, E., Gibon, V., De Greyt, W., Wouters, J., Foubert, I., & Dewettinck, K. (2010). On the fractional crystallization of palm olein : Solid solutions and eutectic solidification. *Food Research International*, *43*, 972–981.

Daels, E., Foubert, I., & Goderis, B. (2017). The effect of adding a commercial phytosterol ester mixture on the phase behavior of palm oil. *Food Research International*, *100*, 841–849.

Danthine, S., & Deroanne, C. (2003). Blending of Hydrogenated Low-Erucic Acid Rapeseed Oil, Low-Erucic Acid Rapeseed Oil, and Hydrogenated Palm Oil or Palm Oil in the Preparation of Shortenings. *Journal of the American Oil Chemists' Society*, *80*(11), 1069–1075.

Dierking, I. (2003). *Textures of Liquid Crystals* (first edit). Weinheim, Germany: Wiley-VCH.

Fernandes, P., & Cabral, J. M. S. (2007). Phytosterols: Applications and recovery methods. *Bioresource Technology*, *98*(12), 2335–2350.

Foubert, I., Dewettinck, K., Van de Walle, D., Dijkstra, A. J., & Quinn, P. J. (2007). Physical Properties: Structural and Physical Characteristics. In F. D. Gunstone, J. L. Harwood, & A. J. Dijkstra (Eds.), *The Lipid Handbook* (3rd ed., pp. 471–534). Boca Raton, USA: CRC Press.

Ginsburg, G. S., Atkinson, D., & Small, D. M. (1984). Physical Properties of Cholesteryl Esters. *Progress in Lipid Research*, *23*, 135–167.

Gommes, C. J., & Goderis, B. (2010). CONEX, a program for angular calibration and averaging of two-dimensional powder scattering patterns. *Journal of Applied Crystallography*, *43*(2), 352–355.

Leeson, P., & Flöter, E. (2002). Solidification behaviour of binary sitosteryl esters mixtures. *Food Research International*, *35*, 983–991.

Man, Y. B. C., Haryati, T., Ghazali, H. M., & Asbi, B. A. (1999). Composition and Thermal Profile of Crude Palm Oil and Its Products. *Journal of the American Oil Chemists' Society*, *76*(2), 237–242.

Martini, S., Herrera, M. L., & Hartel, R. W. (2002). Effect of cooling rate on crystallization behavior of milk fat fraction/sunflower oil blends. *Journal of the American Oil Chemists' Society*, *79*(11), 1055–1062.

Miskandar, M. S., Man, Y. C., Yusoff, M. S. A., & Rahman, R. A. (2005). Quality of margarine: fats selection and processing parameters. *Asia Pacific Journal of Clinical Nutrition*, *14*(4), 387–95.

Moziar, C., DeMan, J. M., & DeMan, L. (1989). Effect of Tempering on the Physical Properties of Shortening. *Canadian Institute of Food Science and Technology Journal*, *22*(3), 238–242.

Narine, S. S., & Marangoni, A. G. (1999). Relating structure of fat crystal networks to mechanical properties: a review. *Food Research International*, *32*, 227–248.

Ntanios, F. (2001). Plant sterol-ester-enriched spreads as an example of a new functional food. *European Journal of Clinical Nutrition*, *103*, 102–106.

Ostlund, R. E. (2007). Phytosterols, cholesterol absorption and healthy diets. *Lipids*, *42*, 41–5.

Pande, G., Akoh, C. C., & Lai, O. M. (2012). Food uses of palm oil and its components. In O. M. Lai, C. P. Tan, & C. C. Akoh (Eds.), *Palm oil. Production, processing, characterization and uses* (2nd ed., pp. 561–586). Urbana, USA: AOCS Press.

Panpipat, W., Xu, X., & Guo, Z. (2013). Improved acylation of phytosterols catalyzed by Candida antarctica lipase A with superior catalytic activity. *Biochemical Engineering Journal*, *70*, 55–62.

Peyronel, F., & Marangoni, A. G. (2014). In search of confectionary fat blends stable to heat: Hydrogenated palm kernel oil stearin with sorbitan monostearate. *Food Research International*, *55*, 93–102.

Piironen, V., Lindsay, D. G., Miettinen, T. A., Toivo, J., & Lampi, A. (2000). Review Plant sterols : biosynthesis, biological function and their importance to human nutrition. *Journal of the Science of Food and Agriculture*, *80*, 939–966.

Ras, R. T., Geleijnse, J. M., & Trautwein, E. A. (2014). LDL-cholesterol-lowering effect of plant sterols and stanols across different dose ranges: a meta-analysis of randomised controlled studies. *British Journal of Nutrition*, *112*, 214–219.

Rodrigues, J. N., Torres, R. P., Mancini-Filho, J., & Gioielli, L. A. (2007). Physical and chemical properties of milkfat and phytosterol esters blends. *Food Research International*, *40*(6), 748–755.

Rousseau, D., Marangoni, A. G., & Jeffrey, K. R. (1998). The Influence of Chemical Interesterification on the Physicochemical Properties of Complex Fat Systems 2: Morphology and Polymorphism, 1833–1839.

Ryckebosch, E., Bruneel, C., Termote-Verhalle, R., Goiris, K., Muylaert, K., & Foubert, I. (2012). Nutritional evaluation of microalgae oils rich in omega-3 long chain polyunsaturated fatty acids as an alternative for fish oil. *Food Chemistry*, *160*, 393–400.

Ryckebosch, E., Muylaert, K., & Foubert, I. (2012). Optimization of an Analytical Procedure for Extraction of Lipids from Microalgae. *Journal of the American Oil Chemists' Society*, *89*, 189–198.

Sato, K. (1999). Solidification and phase transformation behaviour of food fats – a review. *Fett/Lipid*, *12*, 467–474.

Sato, K. (2001). Crystallization behaviour of fats and lipids — a review. *Chemical Engineering Science*, *56*(7), 2255–2265.

Tan, C. P., & Nehdi, I. A. (2012). The physicochemical properties of palm oil and its components. In O. M. Lai, C. P. Tan, & C. C. Akoh (Eds.), *Palm oil. Production, processing, characterization and uses* (2nd ed., pp. 377–392). Ur: AOCS Press.

Timms, R. E. (2003). Confectionery Fats Handbook. Oily Press.

Vaikousi, H., Lazaridou, A., Biliaderis, C. G., & Zawistowski, J. (2007). Phase transitions, solubility, and crystallization kinetics of phytosterols and phytosterol-oil blends. *Journal of Agricultural and Food Chemistry*, *55*(5), 1790–8.

Vereecken, J., Foubert, I., Smith, K. W., & Dewettinck, K. (2007). Relationship between crystallization behavior, microstructure, and macroscopic properties in trans-containing and trans-free filling fats and fillings. *Journal of Agricultural and Food Chemistry*, *55*(19), 7793–801.

Verstringe, S., Danthine, S., Blecker, C., Depypere, F., & Dewettinck, K. (2013). Influence of monopalmitin on the isothermal crystallization mechanism of palm oil. *Food Research International*, *51*(1), 344–353.

Vu, P.-L., Shin, J.-A., Lim, C.-H., & Lee, K.-T. (2004). Lipase-catalyzed production of phytosteryl esters and their crystallization behavior in corn oil. *Food Research International*, *37*(2), 175–180.

Yap, P. H., DeMan, J. M., & DeMan, L. (1989). Polymorphism of palm oil and palm oil products. *Journal of the American Oil Chemists Society*, *66*(5), 693–697.

Figures Captions

Figure 1. Melting curves of phytosterol ester (PE) - palm oil (PO) blends in the 'equilibrium' state as a function of the PE mass fraction (X_{PE}). The grey solid line indicates T_{offset} of the blends as reported by Daels et al. (2017) and measured by synchrotron XRD.

Figure 2. Wide angle X-ray diffraction (A) and small angle X-ray scattering (B) patterns of some phytosterol ester (PE) - palm oil (PO) blends in the 'equilibrium' state.

Figure 3: Images of the lipid crystal networks of different phytosterol ester (PE) - palm oil (PO) blends in the 'equilibrium' state. White bars represent 50 or 100 µm.

Figure 4. Mean melting enthalpy (ΔH) ± standard deviation (n = 5) of phytosterol ester (PE) - palm oil (PO) blends in the 'equilibrium' state as a function of the PE concentration. The black solid line represents the theoretical value of ΔH if PO would have been blended with a fully liquid oil, instead of PE. The grey solid line represents the theoretical value of ΔH if PE would have been blended with a fully liquid oil, instead of PO. The black dotted line is the sum of the two previous ones showing the theoretical value of ΔH of the PE-PO blends supposing both components crystallized.

Figure 5. Mean solid fat content (SFC) ± standard deviation (n = 5) of phytosterol ester (PE) - palm oil (PO) blends in the 'equilibrium' state (black dots) as a function of the PE concentration and of the pure PEs that was subsequently heated to 25°C and kept at 25°C for 1h after reaching the 'equilibrium' state (black square). The black solid line represents the theoretical value of SFC if PO would have been blended with a fully liquid oil, instead of PE. The grey solid line represents the theoretical value of SFC if PE_x would have been blended with a fully liquid oil, instead of PO. The black dotted line shows the theoretical value of the SFC of the PE-PO blends supposing they both crystallized, but the PE solids consisting only of PE_x.

Figure 6: Mean hardness ± standard deviation (n = 4) of phytosterol ester (PE) - palm oil (PO) blends in the 'equilibrium' state

Figure 1

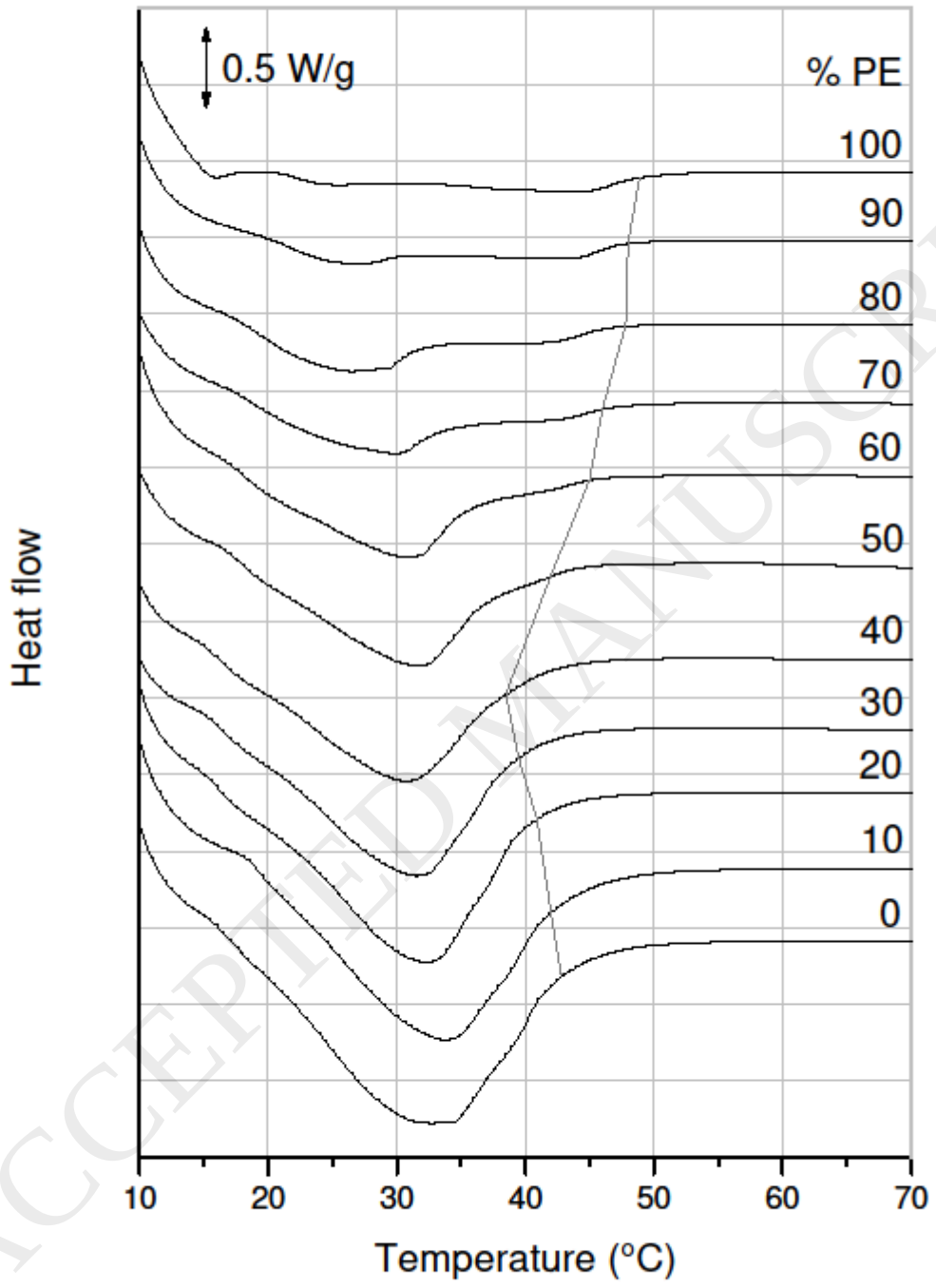

Fig 2

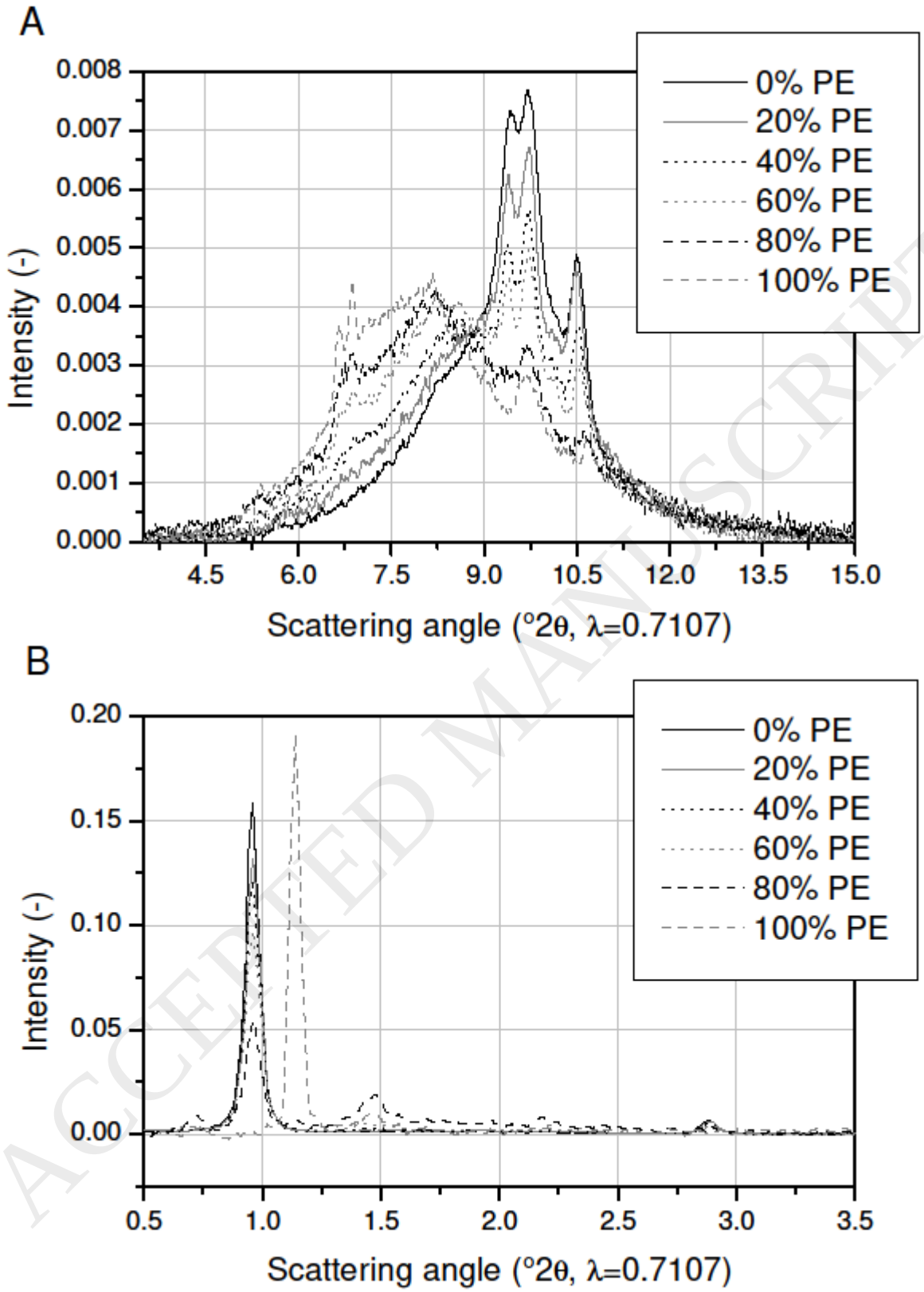

Fig 3

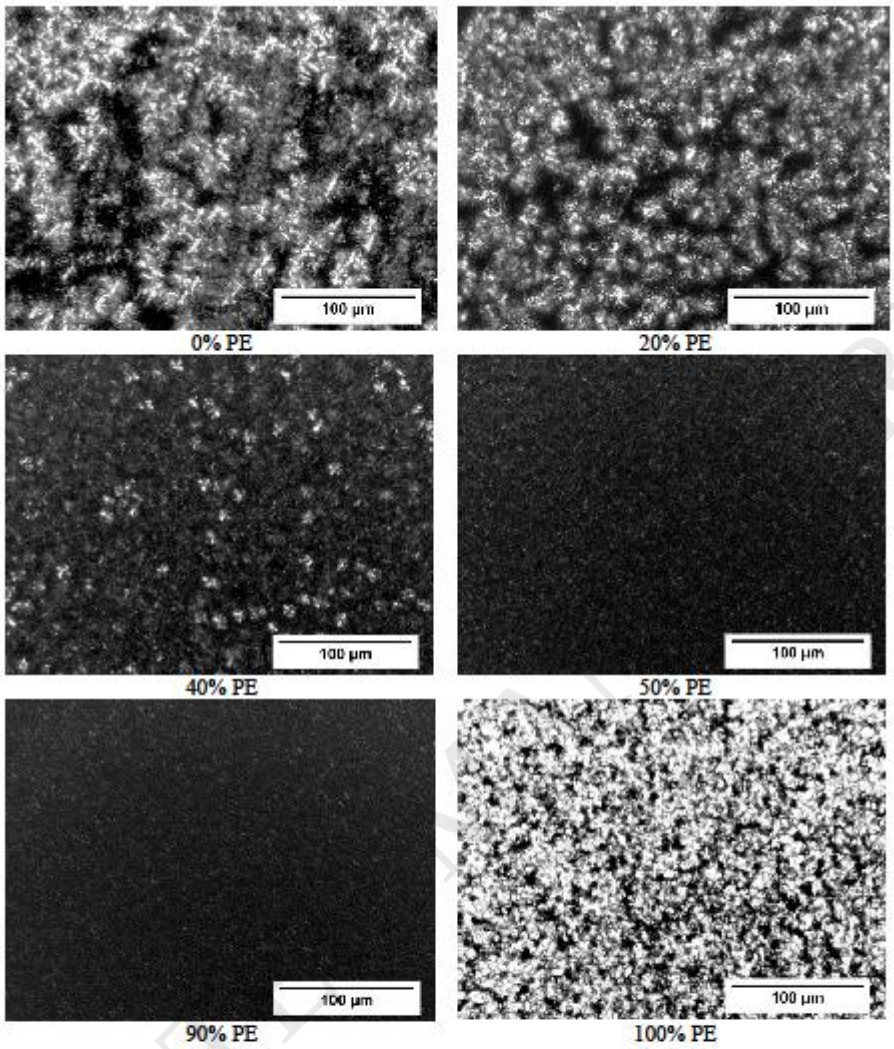

Fig 4

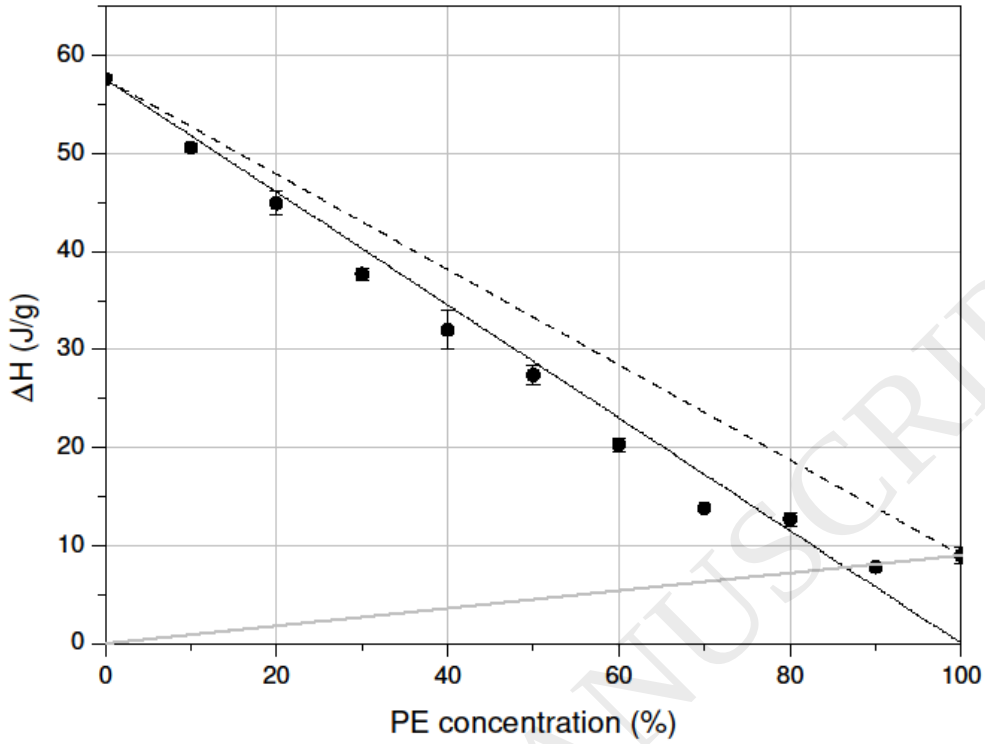

Fig 5

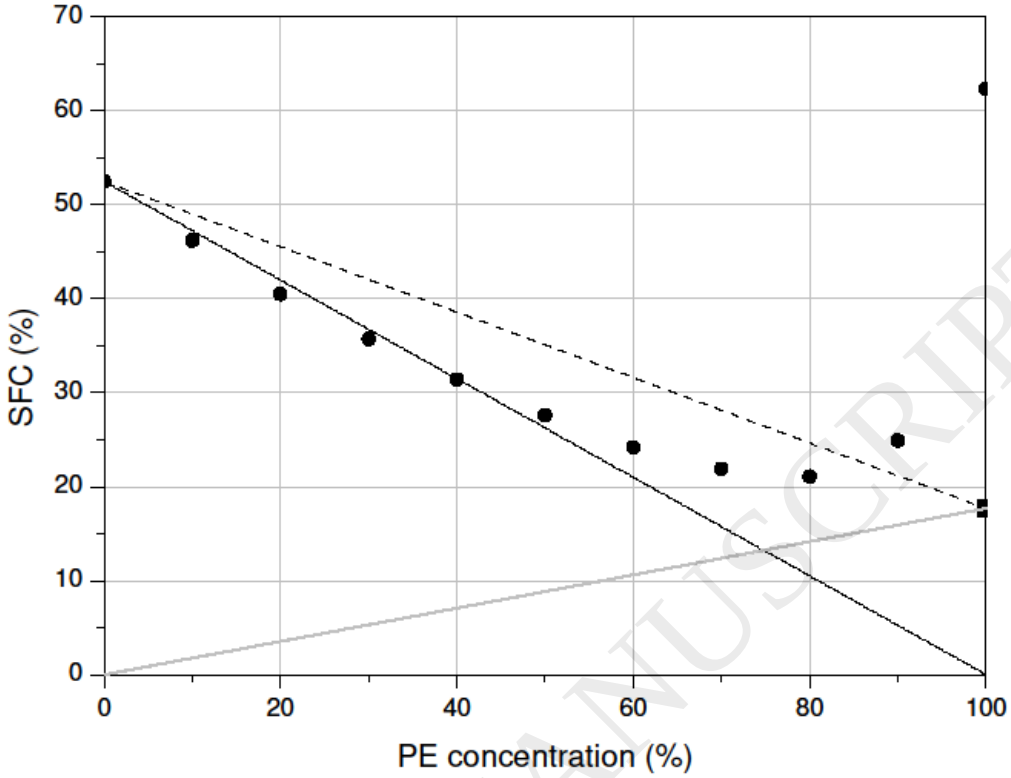

Fig 6

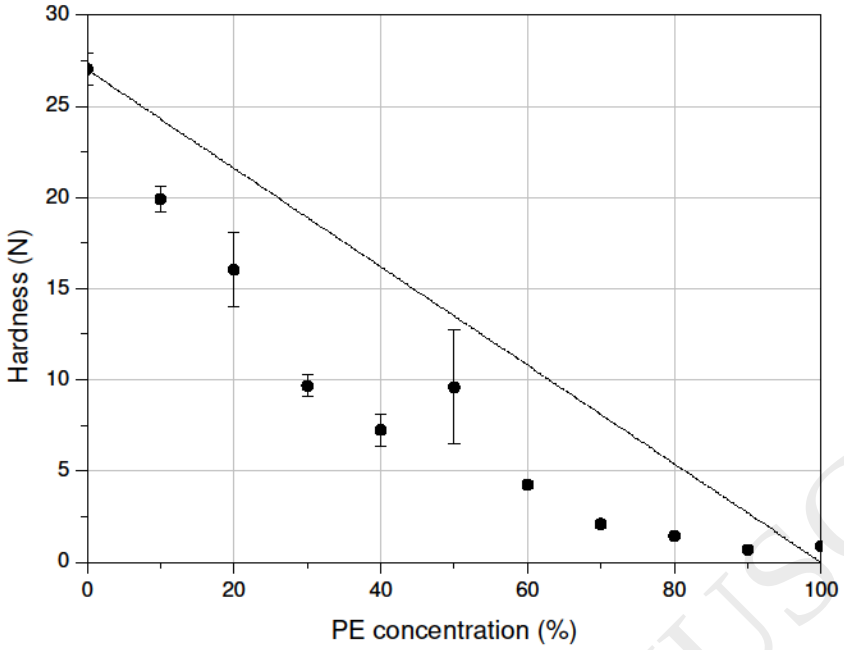

Tables

Table 1. Sterol composition (%) of the commercial phytosterol ester mixture. The values show the average of two measurements. The error is 0.2%.

Sterol	
Brassicasterol	1.3
Campesterol	10.0
Stigmasterol	0.6
β-sitosterol	78.5
β-sitostanol	9.7

Table 2. Fatty acid composition (%) of palm oil and the commercial phytosterol ester mixture. The values show the average of three measurements. The error is 0.2%.

Fatty acid	Palm oil	Phytosterol ester mixture
C14:0	1.0	-
C16:0	45.4	6.6
C18:0	4.3	3.8
C18:1	39.6	29.8
C18:2	9.8	59.7

Table 3. Triglyceride (TAG) composition (%) of palm oil. The values show the average of two measurements. The error is 0.02%. Abbreviations: L: linoleic acid, O: oleic acid, P: palmitic acid, M: myristic acid, S: stearic acid

TAG	
PLL	2.71
MLP	0.67
OOL	1.87
POL	10.97
PLP	10.54
OOO	3.62
POO	23.14
POP	31.42
PPP	5.15
SOO	2.49
POS	5.64
PPS	1.08
SOS	0.70